

Non-equilibrium steady state and induced currents of a mesoscopically-glassy system: interplay of resistor-network theory and Sinai physics

Daniel Hurowitz¹, Saar Rahav², Doron Cohen¹

¹*Department of Physics, Ben-Gurion University of the Negev, Beer-Sheva, Israel*

²*Schulich Faculty of Chemistry, Technion - Israel Institute of Technology, Haifa 32000, Israel*

We introduce an explicit solution for the non-equilibrium steady state (NESS) of a ring that is coupled to a thermal bath, and is driven by an external hot source with log-wide distribution of couplings. Having time scales that stretch over several decades is similar to glassy systems. Consequently there is a wide range of driving intensities where the NESS is like that of a random walker in a biased Brownian landscape. We investigate the resulting statistics of the induced current I . For a single ring we discuss how $\text{sign}(I)$ fluctuates as the intensity of the driving is increased, while for an ensemble of rings we highlight the fingerprints of Sinai physics on the $\text{abs}(I)$ distribution.

The transport in a chain due to random non-symmetric transition probabilities is a fundamental problem in statistical mechanics [1–5]. It can be regarded as a *random walk in a random environment* [6, 7]. This type of dynamics is of great relevance for surface diffusion [8], thermal ratchets [9–12] and was used to model diverse biological systems, such as molecular motors, enzymes, and unidirectional motion of proteins along filaments [13–16]. Of particular interest are applications that concern the conduction of DNA segments [17, 18], and thin glassy electrolytes under high voltages [19–24].

Mathematically one can visualize the dynamics as a random-walk of a particle that makes incoherent jumps between “sites” in a network. In an unbounded quasi-one-dimensional network we might have either diffusion or sub-diffusive Sinai spreading [6], depending on whether the transitions rates form a symmetric matrix or not. In contrast, when the system is bounded it eventually reaches a well-defined steady state. This would be an equilibrium *canonical* (Boltzmann) state if the transition rates were detailed-balanced, else it is termed non-equilibrium steady state (NESS).

We would like to consider the NESS of a mesoscopically glassy system. By “glassiness” we mean that the rates that are induced by a bath, or by an external source, have a log-wide distribution of transition rates, hence many time scales are involved. Specifically we consider a common way of maintaining a NESS (Fig.1): a system that is coupled to a driving source (“hot bath”) that spoils the detailed-balance of the environment (“cold bath”). The log wide distribution of the transition rates leads to a novel NESS. In previous publications we have pointed out that due to “glassiness” (also termed “sparsity”) the physics of Sinai-type disorder is a relevant ingredient in the analysis of energy absorption [25] and transport [26].

Scope.— Below we introduce an explicit NESS solution for a minimal model that has all the essential ingredients of the problem, involving transitions between sites on a ring and a log-wide distribution of couplings to an external driving source. The induced steady state current I is the central quantity used to characterize the

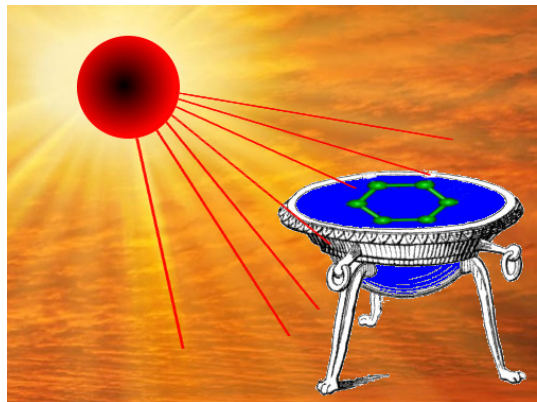


FIG. 1: A ring made up of N sites is immersed in a “cold” bath and subjected to a “hot” driving source [a]. As a result a current is induced. In the numerics the the driving source induces rates that are log-box distributed over 6 decades.

NESS in actual experiments. The purpose of the present study is to investigate its statistics. Specifically, for a single ring we discuss how $\text{sign}(I)$ fluctuates as the intensity of the driving is increased, while for an ensemble of rings we highlight the fingerprints of Sinai physics on the $\text{abs}(I)$ distribution.

Remarks.— Previous study of Sinai-type disordered systems [7], has considered an open geometry with uncorrelated transition rates that have the same coupling everywhere. Consequentially the random-resistor-network aspect (which is related to local variation of the couplings) has not emerged. Furthermore, in the physically motivated setup that we have defined above (ring+bath+driving) Sinai physics would not arise if the couplings to the driving source were merely disorderly random. The log-wide distribution is a crucial ingredient. Finally, in a closed (ring) geometry, unlike an open (two terminal) geometry, the statistics of I is not only affected by the distribution of transition rates, but also by the spatial profile of the NESS. This is like “canonical” as opposed to “grand canonical” setting, leading to remarkably different results.

The model.— Consider a ring that consists of sites labeled by n with positions $x = n$ that are defined modulo N . The bonds are labeled as $\vec{n} \equiv (n-1 \rightsquigarrow n)$. The inverse bond is \overleftarrow{n} , and if direction does not matter we label both by \bar{n} . The position of the n th bond is defined as $x_n \equiv n-(1/2)$. The on-site energies E_n are normally distributed over a range Δ , and the transitions rates are between nearest-neighboring sites:

$$w_{\vec{n}} = w_{\vec{n}}^\beta + \nu g_{\bar{n}} \quad (1)$$

Here w^β are the rates that are induced by a bath that has a finite temperature T_B . The $g_{\bar{n}}$ are couplings to a driving source that has an intensity ν . These coupling are log-box distributed within $[g_{\min}, g_{\max}]$. This means that $\ln(g_{\bar{n}})$ are distributed uniformly over a range $\sigma = \ln(g_{\max}/g_{\min})$. The bath transition rates satisfy detailed-balance, namely $w_{\vec{n}}^\beta/w_{\overleftarrow{n}}^\beta = \exp[-(E_n - E_{n-1})/T_B]$. The driving spoils the detailed-balance. We define the resulted stochastic field as follows:

$$\mathcal{E}(x_n) \equiv \ln \left[\frac{w_{\vec{n}}}{w_{\overleftarrow{n}}} \right] \approx - \left[\frac{1}{1 + g_{\bar{n}}\nu} \right] \frac{E_n - E_{n-1}}{T_B} \quad (2)$$

where the last equality assumes $\Delta \ll T_B$, and without loss of generality the $g_{\bar{n}}$ have been re-scaled such that all the bath-induced transitions have the same average transition rate $\bar{w}^\beta = 1$.

The direction of the current.— The stochastic motive force (SMF), also known as the affinity, or as the entropy production [27–30] determines $\text{sign}(I)$. It is defined as follows:

$$\mathcal{E}_\odot \equiv \ln \left[\frac{\prod_n w_{\vec{n}}}{\prod_n w_{\overleftarrow{n}}} \right] = \oint \mathcal{E}(x) dx \quad (3)$$

Using Eq.(2) one observes that for $\nu \ll g_{\max}^{-1}$ the SMF is linear $\mathcal{E}_\odot \propto \nu$, while for $\nu \gg g_{\min}^{-1}$ it vanishes $\mathcal{E}_\odot \propto 1/\nu$. In the intermediate regime, which we call below *the Sinai regime*, the SMF changes sign several times, see Fig.2. Using the notations

$$\tau \equiv \frac{1}{\sigma} \ln(g_{\max}\nu) \quad (4)$$

and $\tau_n = (1/\sigma) \ln(g_{\max}/g_{\bar{n}})$, the expression for the SMF takes the following form:

$$\mathcal{E}_\odot(\tau) = - \sum_{n=1}^N f_\sigma(\tau - \tau_n) \frac{E_n - E_{n-1}}{T_B} \quad (5)$$

where $f_\sigma(t) \equiv [1 + e^{\sigma t}]^{-1}$ is like a step function. If $f(t)$ were a sharp step function it would follow that in the Sinai regime $\mathcal{E}_\odot(\tau)$ is formally like a random walk. The number of sign reversals equals the number of times the random walker cross the origin. We have here a coarse-grained random walk: the τ_n are distributed uniformly over a range $[0, 1]$, and each step is smoothed by $f_\sigma(t)$

such that the effective number of coarse-grained steps is σ . Hence we expect the number of sign change to be not $\sim \sqrt{\pi N}$ [31, 32] but $\sim \sqrt{\pi \sigma}$, reflecting the log-width of the distribution.

Adding bonds in series.— The NESS equations are quite simple and can be solved using elementary algebra as in [19, 20, 24, 26], or optionally using the network formalism for stochastic systems [34–36]. Below we propose a generalized resistor-network approach that allows to obtain a more illuminating version for the NESS, that will provide a better insight for the statistical analysis. Let us assume that we have a NESS with a current I . The steady state equations for two adjacent bonds are

$$I = w_{\vec{1}} p_0 - w_{\overleftarrow{1}} p_1 \quad (6)$$

$$I = w_{\vec{2}} p_1 - w_{\overleftarrow{2}} p_2 \quad (7)$$

We can combine them into one equation:

$$I = \vec{G} p_0 - \overleftarrow{G} p_2, \quad \vec{G} \equiv \left[\frac{1}{w_{\vec{1}}} + \frac{1}{w_{\vec{2}}} \left(\frac{w_{\overleftarrow{1}}}{w_{\vec{1}}} \right) \right]^{-1} \quad (8)$$

and similar expression for \overleftarrow{G} . We can repeat this procedure iteratively. If we have N bonds in series we get

$$\vec{G} = \left[\sum_{m=1}^N \frac{1}{w_{\vec{m}}} \exp \left(- \int_0^{m-1} \mathcal{E}(x) dx \right) \right]^{-1} \quad (9)$$

Coming back to the ring, we can cut it at an arbitrary site n , and calculate the associated G s. It follows that $I = (\vec{G}_n - \overleftarrow{G}_n) p_n$. Consequently the NESS is

$$p_n = \frac{I}{\vec{G}_n - \overleftarrow{G}_n} \quad (10)$$

and I can be regarded as the normalization factor:

$$I = \left[\sum_{n=1}^N \frac{1}{\vec{G}_n - \overleftarrow{G}_n} \right]^{-1} \quad (11)$$

In the next paragraph we show how to write these results in an explicit way that illuminates the relevant physics.

The NESS formula.— We define the conductance of a bond as the geometric mean of the clockwise and anticlockwise transmission rates:

$$w(x_n) = \sqrt{w_{\vec{n}} w_{\overleftarrow{n}}} \quad (12)$$

Hence $w_{\vec{n}} = w(x_n) \exp[(1/2)\mathcal{E}(x_n)]$. Accordingly

$$\vec{G}_n = \left[\sum_{m=n+1}^{N+n} \frac{1}{w(x_m)} \exp \left(- \int_n^{x_m} \mathcal{E}(x) dx \right) \right]^{-1} \quad (13)$$

With the implicit understanding that the summation and the integration are anticlockwise modulo N . With the new notations it is easy to see that $\overleftarrow{G}_n = \exp(-\mathcal{E}_\odot) \vec{G}_n$.

We use the notation G_n for the geometric mean. Consequently the formula for the current takes the form

$$I = \left[\sum_{n=1}^N \frac{1}{G_n} \right]^{-1} 2 \sinh \left(\frac{\mathcal{E}_\odot}{2} \right) \quad (14)$$

while $p_n \propto 1/G_n$. Our next task is to work out a tangible expression for the latter. Regarding x as an extended coordinate the potential $V(x)$ that is associated with the field $\mathcal{E}(x)$ is a tilted periodic potential. Adding $[\mathcal{E}_\odot/N]x$ we get a periodic potential $U(x)$, see Fig.3. Accordingly

$$\int_{x'}^{x''} \mathcal{E}(x) dx = U(x') - U(x'') + \frac{\mathcal{E}_\odot}{N} (x'' - x') \quad (15)$$

With any function $A(x)$ we can associate a smoothed version using the following definition

$$\sum_{r=1}^N A(x+r) e^{U(x+r) - (1/N)\mathcal{E}_\odot r} \equiv A_\varepsilon(x) e^{U_\varepsilon(x)} \quad (16)$$

In particular the smoothed potential $U_\varepsilon(x)$ is defined by this expression with $A = 1$. Note that without loss of generality it is convenient to have in mind $\mathcal{E}_\odot > 0$. (One can always flip the x direction). Note also that the smoothing scale N/\mathcal{E}_\odot becomes larger for smaller SMF. With the above definitions we can write the NESS expression as follows:

$$p_n \propto \left(\frac{1}{w(x_n)} \right)_\varepsilon e^{-(U(n) - U_\varepsilon(n))} \quad (17)$$

This expression is physically illuminating, see Fig.3. In the limit of zero SMF it coincides, as expected, with the canonical (Boltzmann) result. For finite SMF the smoothed pre-factor and the smoothed potential are not merely constants. Accordingly the pre-exponential factor becomes important and the “slow” modulation by the Boltzmann factor is flattened. If we take the formal limit of infinite SMF the Boltzmann factor disappears and we are left with $p_n \propto 1/w_n$ as expected from the continuity equation for a resistor-network.

Statistics of the current.— From the preceding analysis it should become clear that the formula for the current can be written schematically as

$$I(\nu) \sim \frac{1}{N} w_\varepsilon e^{-B} 2 \sinh \left(\frac{\mathcal{E}_\odot}{2} \right) \quad (18)$$

In the absence of a potential landscape ($U(x) = 0$) the formula becomes equivalent to Ohm law: it is a trivial exercise to derive it if all anticlockwise and clockwise rates are equal to the same values \vec{w} and \overleftarrow{w} respectively, hence $w_\varepsilon = (\vec{w}\overleftarrow{w})^{1/2}$, and $\mathcal{E}_\odot = N \ln(\vec{w}/\overleftarrow{w})$. In the presence of a potential landscape we have an activation barrier. Assuming that the current is dominated by the highest peak a reasonable estimate would be

$$B = \max \{U(x) - U_\varepsilon(x)\} \approx \frac{1}{2} [\max\{U\} - \min\{U\}] \quad (19)$$

The implication of Eq.(18) with Eq.(19) for the *statistics* of the current is as follows: in the Sinai regime we expect that it will reflect the *log-wide* distribution of the activation factor, as discussed below, while outside of the Sinai regime we expect it to reflect the *normal* distributions of the total resistance w_ε^{-1} , and of the SMF.

Statistics in the Sinai regime.— We now focus on the statistics in the Sinai regime. In order to unfold the log-wide statistics it is not a correct procedure to plot blindly the distribution of $\ln(|I|)$. Rather one should look on the joint distribution (\mathcal{E}_\odot, I) . See Fig.4a. The non-trivial statistics is clearly apparent. In order to describe it analytically we use the single-barrier estimate of Eq.(19), which is tested in Fig.4b. We see that it overestimates the current for small B values (flat landscape) as expected, but it can be trusted for large B where the Sinai physics becomes relevant.

In an actual experiment it would be desired to extract the statistics from the $I(\nu)$ measurements without referring to the SMF. See Fig.5. Either way this figure confirms that the I statistics is the same as the barrier $\exp(-B)$ statistics. We therefore turn to find an explicit expression for the latter. The probability to have a random walk trajectory $X_n = U(x_n)$ within $[X_a, X_b]$ equals the survival probability of a diffusing process that starts as a delta function at $X = 0$ with absorbing boundary conditions at X_a and X_b . Integrating over all possible positions of the walls such that $X_b - X_a = 2B$ is like starting with a uniform distribution between the walls. From here it is straightforward to deduce [b]

$$\text{Prob}\{\text{barrier} < B\} \sim \exp \left[-\frac{1}{2} \left(\frac{\pi \sigma_U}{2B} \right)^2 \right] \quad (20)$$

where $\sigma_U^2 = 2DN$ is the variance of the diffusing ‘points’, which is determined by the diffusion coefficient $D \propto \Delta^2$. Taking into account that for a given ν a fraction of the elements in Eq.(5) are effectively zero we get

$$\sigma_U^2 = 2\Delta^2 N \frac{\ln(g_{\max}\nu)}{\sigma} \quad (21)$$

The validity of the exact version of Eq.(20), see [b], has been verified in Fig.4. No fitting parameters are required.

Summary.— We have introduced a generalized “random-resistor-network” approach for the purpose of obtaining the NESS current due to nonsymmetric transition rates. Specifically our interest was focused on the NESS of a “glassy” mesoscopic system. The NESS expression clearly interpolates the canonical (Boltzmann) result that applies in equilibrium, with the resistor-network result, that applies at infinite temperature. Due to the “glassiness” the current has novel dependence on the driving intensity, and it possesses unique statistical properties that reflect the Brownian landscape of the stochastic potential. This statistics is related to Sinai’s random walk problem, and would not arise if the couplings to the driving source were merely disordered.

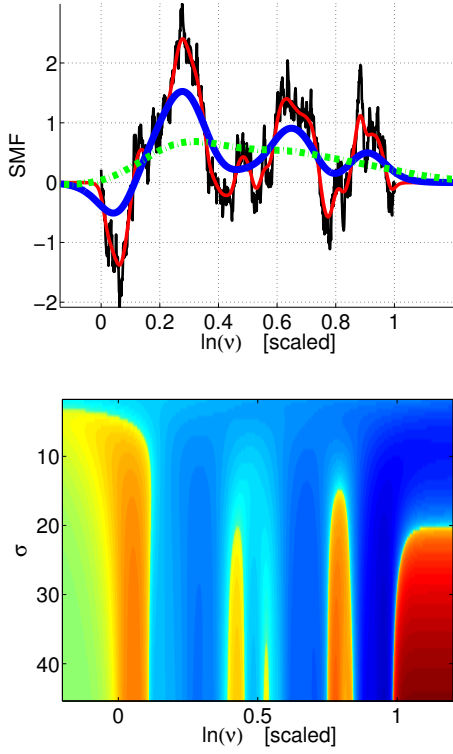


FIG. 2: We consider a ring with $N = 1000$ sites whose energies are normally distributed with dispersion $\Delta = 1$. The bath temperature is $T_B = 10$. In the upper panel the SMF of Eq. (5) is plotted for $\sigma = \infty$, and for $\sigma = 50, 10, 4$. The smaller σ , the smoother ν dependence. This is reflected in the current $I(\nu)$, which is imaged in the lower panel. In both panels the horizontal axis is the scaled driving intensity as defined in Eq. (4).

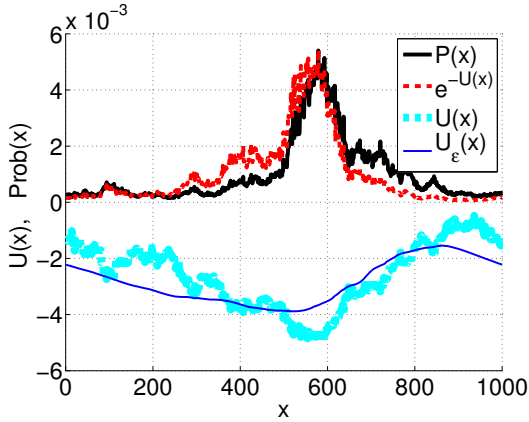


FIG. 3: The NESS profile of Eq. (17) (solid black) is similar but not identical to the quasi-equilibrium distribution (dashed red line). Also shown (lower curves) is the potential landscape $U(x)$ and its smoothed version $U_\epsilon(x)$. The parameters are the same as in Fig. 2, however the bonds were rearranged to have a larger SMF, namely $\mathcal{E}_\odot = 7.4$. The driving intensity corresponds to $\tau = 0.3$.

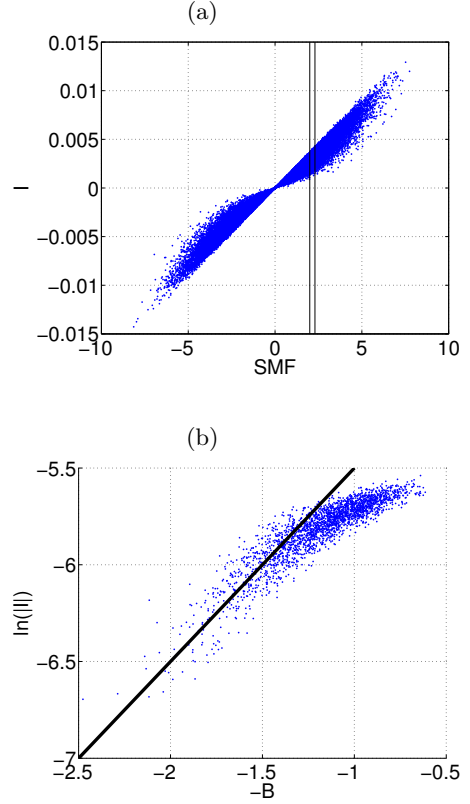


FIG. 4: (a) Scatter diagram of the current versus the SMF in the Sinai regime. Note that in the linear regime, see [b], it looks like a perfect linear correlation with *negligible* transverse dispersion. (b) The correlation between the current I and the barrier B , within the slice $\mathcal{E}_\odot \in [2.0, 2.1]$. One deduces that the single-barrier approximation is valid for small currents.

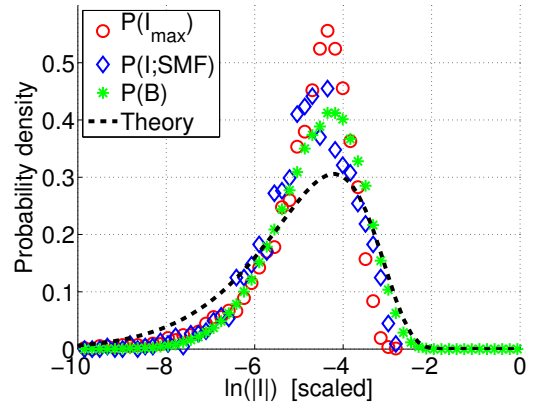


FIG. 5: The log-wide distribution $P(I)$ of the current in the Sinai regime is revealed provided a proper procedure is adopted. For theoretical analysis it is convenient to plot an histogram of the I values for a given SMF: the blue diamonds refer to the data of Fig. 4b. In an actual experiment it is desired to extract statistics from $I(\nu)$ measurements without referring to the SMF: the red empty circles show the statistics of the first maximum of $I(\nu)$. Both distributions look the same, and reflect the barrier statistics (full green circles). The line is the exact version [b] of Eq. (21).

Acknowledgments.— This research was supported by the Israel Science Foundation (grant No.29/11). We thank Oleg Krichevsky (BGU) for a useful advice. SR is grateful for support from the Israel Science Foundation (grant 924/11).

-
- [1] B. Derrida, Y. Pomeau, Phys. Rev. Lett. 48, 627 (1982).
 - [2] S. H. Noskowitz, I. Goldhirsch, Phys. Rev. Lett. 61, 500 (1988); Phys. Rev. A 42, 2047 (1990).
 - [3] J. P. Bouchaud, A. Comtet, A. Georges, P. Le Doussal, Ann. Phys. (N.Y.) 201, 285 (1990).
 - [4] H. E. Roman, M. Schwartz, A. Bunde, S. Havlin, Europhys. Lett. 7, 389 (1988).
 - [5] S.F. Burlatsky, G.S. Oshanin, A.V. Mogutov, M. Moreau, Phys. Rev. A 45, R6955 (1992).
 - [6] Ya. G. Sinai, Theory Probab. Appl. 27, 247 (1982).
 - [7] S.F. Burlatsky, G.S. Oshanin, A.V. Mogutov, M. Moreau, Phys. Rev. A 45, R6955 (1992).
 - [8] R. L. Schwoebel and E. J. Shipsey, J. Appl. Phys. 37, 3682 (1966)
 - [9] M. O. Magnasco, Phys. Rev. Lett. 71, 1477 (1993)
 - [10] R. D. Astumian and M. Bier, Phys. Rev. Lett. 72, 1766 (1994)
 - [11] M. O. Magnasco, Phys. Rev. Lett. 72, 2656 (1994)
 - [12] P. Reimann, Phys. Rep. 361, 57 (2002)
 - [13] C.T. MacDonald, J.H. Gibbs and A.C. Pipkin, Biopolymers, 6, 1 (1968)
 - [14] H. X. Zhou and Y. D. Chen, Phys. Rev. Lett. 77, 194 (1996)
 - [15] E. Frey and K. Kroy, Ann. Phys. 14, 20 (2005)
 - [16] A.B. Kolomeisky and M.E. Fisher, Annu. Rev. Phys. Chem. 58, 675 (2007)
 - [17] B. Xu, P. Zhang, X. Li and N. Tao, Nano Lett. 4, 1105 (2004)
 - [18] H. W. Fink and C. Schönenberger, Nature 398, 407 (1999)
 - [19] K. W. Kehr, K. Mussawisade, and T. Wichmann, Phys. Rev. E 56, R2351 (1997).
 - [20] A. Heuer, S. Murugavel, and B. Roling, Phys. Rev. B 72, 174304 (2005).
 - [21] S. Murugavel and B. Roling, J. Non-Cryst. Solids 351, 2819 (2005).
 - [22] A. Heuer, S. Murugavel and B. Roling, Phys. Rev. B, 72, 174304 (2005).
 - [23] B. Roling, S. Murugavel, A. Heuer, L. Luhning, R. Friedrich and S. Rothel, Phys. Chem. Chem. Phys. 10, 4211 (2008).
 - [24] M. Einax, M. Korner, P. Maass, A. Nitzan, Phys. Chem. Chem. Phys. 12, 645 (2010). in ring systems and open channels
 - [25] D. Hurowitz, D. Cohen, Europhysics Letters 93, 60002 (2011)
 - [26] D. Hurowitz, S. Rahav, D. Cohen, Europhysics Letters 98, 20002 (2012)
 - [27] J.L. Lebowitz, H. Spohn, J. Stat. Mech, v95 333 (1999).
 - [28] P. Gaspard, J. Chem. Phys., 120, 8898 (2004).
 - [29] Udo Seifert, Phys. Rev. Lett. 95, 040602 (2005)
 - [30] D. Andrieux and P. Gaspard, J. Stat. Phys., 127, 107 (2007).
 - [31] Adrienne W. Kemp, Advances in Applied Probability , Vol. 19, No. 2 (Jun., 1987), pp. 505-507
 - [32] W. Feller, An Introduction to Probability Theory and its Applications.
 - [33] Meyer Dwass, The Annals of Mathematical Statistics , Vol. 38, No. 4 (Aug., 1967), pp. 1042-1053 **not cited**
 - [34] J. Schnakenberg, Rev. Mod. Phys. 48, 571 (1976).
 - [35] T.L. Hill, J. Theor. Biol. v10, 442 (1966)
 - [36] R.K.P. Zia, B. Schmittmann, J. Stat. Mech., P07012 (2007).
 - [37] P. Kohli, C. C. Harell, Z. Cao, R. Gasparac and R. Martin, Science 305, 984 (2004).
 - [a] This illustration combines pieces of images that were taken from <http://en.wikipedia.org/wiki/Aeolipile> and <http://thehealthyhavenblog.com/2012/06/18/sun-safety>.
 - [b] See supplementary material at URL for some extra technical details **regarding...**

Supplementary Material

DETAILED DEFINITION OF THE MODEL

Form the detailed balance condition it follows that to leading order

$$w_{\vec{n}}^{\beta} \approx \left[1 - \frac{1}{2} \left(\frac{E_n - E_{n-1}}{T_B} \right) \right] \bar{w}_{\vec{n}}^{\beta} \quad (22)$$

$$w_{\bar{n}}^{\beta} \approx \left[1 + \frac{1}{2} \left(\frac{E_n - E_{n-1}}{T_B} \right) \right] \bar{w}_{\bar{n}}^{\beta} \quad (23)$$

It follows that

$$\frac{w_{\vec{n}}}{w_{\bar{n}}} = \frac{w_{\vec{n}}^{\beta} + \nu g_{\bar{n}}}{w_{\bar{n}}^{\beta} + \nu g_{\bar{n}}} \approx 1 + \frac{(E_n - E_{n-1})/T_B}{1 + (g_{\bar{n}}/\bar{w}_{\bar{n}}^{\beta})\nu} \quad (24)$$

Absorbing the bath couplings into the definition of the $g_{\bar{n}}$ we get

$$\mathcal{E}(x_n) \equiv \ln \left[\frac{w_{\vec{n}}}{w_{\bar{n}}} \right] \approx - \left[\frac{1}{1 + g_{\bar{n}}\nu} \right] \frac{E_n - E_{n-1}}{T_B} \quad (25)$$

The SMF is obtained by integrating the stochastic field along the entire ring

$$\mathcal{E}_{\odot} \approx - \sum_{n=1}^N \left[\frac{1}{1 + g_{\bar{n}}\nu} \right] \frac{\Delta_n}{T_B} \quad (26)$$

STATISTICS OF CURRENT OUTSIDE OF THE SINAI REGIME

As the driving intensity is increased one observes a crossover from a linear regime, to a Sinai regime, and finally a saturation regime:

$$\text{Linear regime:} \quad \nu < g_{max}^{-1} \quad (27)$$

$$\text{Sinai regime:} \quad g_{max}^{-1} < \nu < g_{min}^{-1} \quad (28)$$

$$\text{Saturation regime:} \quad \nu > g_{min}^{-1} \quad (29)$$

Consequently we get for the SMF the following approximations:

$$\mathcal{E}_{\odot} \approx \frac{1}{T_B} \begin{cases} \Delta^{(0)}\nu, & \text{Linear regime} \\ -\Delta^{(\infty)}/\nu, & \text{Saturation regime} \end{cases} \quad (30)$$

where

$$\Delta^{(0)} \equiv \sum_n g_{\bar{n}} \Delta_n \sim \pm \left[2N \text{Var}(g) \right]^{1/2} \Delta \quad (31)$$

$$\Delta^{(\infty)} \equiv \sum_n \frac{1}{g_{\bar{n}}} \Delta_n \sim \pm \left[2N \text{Var}(g^{-1}) \right]^{1/2} \Delta \quad (32)$$

The estimates for $\Delta^{(0)}$ and for $\Delta^{(\infty)}$ follow from the observation that we have sums of independent random variables. For example $\Delta^{(0)}$ can be re-arranged as $\sum_{n=1}^N (g_{\bar{n}+1} - g_{\bar{n}}) E_n$. Furthermore, we conclude that both $\Delta^{(0)}$ and $\Delta^{(\infty)}$ have *normal* statistics as implied by the central limit theorem. This implies *normal* statistics for the SMF, and hence for the current, as verified in [Fig.6](#).

RANDOM-WALK OCCUPATION-RANGE STATISTICS

In this section we derived the probability density function $f(R)$ to have a random walk process $x(\cdot)$ of t steps that occupies a range R . This is determined by the probability

$$P_t(x_a, x_b) \equiv \text{Prob}(x_a < x(t') < x_b \text{ for any } t' \in [0, t]) \quad (33)$$

Accordingly the joint probability density that a random walker would occupy an interval $[x_a, x_b]$ is

$$f(x_a, x_b) = -\frac{d}{dx_a} \frac{d}{dx_b} P_t(x_a, x_b) \quad (34)$$

It is convenient to use the coordinates

$$X = \frac{x_a + x_b}{2} \quad (35)$$

$$R = x_b - x_a \quad (36)$$

Consequently the expression for $f(R)$ is

$$f(R) = \int_{-\infty}^0 \int_0^{\infty} dx_a dx_b f(x_a, x_b) \delta(R - (x_b - x_a)) \quad (37)$$

$$f(R) = - \int_{-R/2}^{R/2} \left(\frac{1}{4} \partial_X^2 - \partial_R^2 \right) P_t(R, X) dX \quad (38)$$

Taking into account that $P_t(R, X)$ and its derivatives vanish at the endpoints $X = \pm(R/2)$ we get

$$f(R) = \int_{-R/2}^{R/2} \partial_R^2 P_t(R, X) dX = \partial_R^2 [R P_t(R)] \quad (39)$$

where $P_t(R)$ is the survival probability of a diffusion process that starts with an initial *uniform* distribution, instead of a random walk that starts as a delta distribution. Optionally we can write

$$\text{Prob}(\text{range} < R) = \partial_R [R P_t(R)] \quad (40)$$

We now turn to find an explicit expression for $P_t(R)$. This is done by solving the diffusion equation. Using Fourier expansion the solution is

$$\rho_t(x) = \sum_{n=1,3,5,\dots}^{\infty} \exp \left[-D \left(\frac{\pi n}{R} \right)^2 t \right] \frac{4}{\pi n R} \sin \left(\frac{\pi n}{R} x \right) \quad (41)$$

For simplicity we have shifted above the domain to $x \in [0, R]$. For the survival probability we get

$$P_t(R) = \int_{-R/2}^{R/2} \rho_t(x) dx = \sum_{n=1,3,5,\dots}^{\infty} \frac{8}{\pi^2 n^2} \exp \left[-D \left(\frac{\pi n}{R} \right)^2 t \right] \quad (42)$$

Using Eq.(42) in Eq.(39) we get

$$f(R) = \frac{8\sigma^2}{R^3} \sum_{n=1,3,5,\dots}^{\infty} \left[\left(\frac{\pi \sigma n}{R} \right)^2 - 1 \right] \exp \left[-\frac{1}{2} \left(\frac{\pi \sigma n}{R} \right)^2 \right] \quad (43)$$

This result is in perfect agreement with the numerical simulation of Fig.7. Still we would like to have a more compact expression. One possibility is to keep only the first term. The other possibility is to approximate the summation by an integral:

$$\text{Prob}(\text{range} < R) \approx \frac{2}{\pi^2} \frac{\partial}{\partial R} \left[R \int_1^{\infty} \frac{dx}{x^2} \exp \left(-\frac{\pi^2 D t}{R^2} x^2 \right) \right] = \exp \left(-\frac{\pi^2 D t}{R^2} \right) \quad (44)$$

Either way we get

$$\text{Prob}(\text{range} < R) \sim \exp \left(-\frac{1}{2} \left(\frac{\pi \sigma}{R} \right)^2 \right) \quad (45)$$

where $\sigma^2 = 2Dt$. This asymptotic expression is illustrated in Fig.7. Though it does not work very well, it has the obvious advantage of simplicity.

RANDOM-WALK MAXIMAL-DISTANCE STATISTICS

The occupation-range statistics of the previous section should not be confused with the maximal-distance statistics. The maximal distance from the initial point is defined as follows:

$$K = \max[x(t)], \quad \text{where } 0 < t < N \quad (46)$$

Naively, one might think that the distribution of K is similar to the distribution of R . But this is not true. The exact result is [33]

$$\text{Prob}(K \geq k; N) = \frac{\binom{2N}{N-k}}{\binom{2N}{N}}, \quad k = 0, 1, 2 \dots N \quad (47)$$

Switching variables to $\kappa = k/N$ and taking the large N limit, one obtains the probability density function

$$f(\kappa) = N \left[\frac{(1-\kappa)^{\kappa-1}}{(1+\kappa)^{\kappa+1}} \right]^N \ln \left[\frac{1+\kappa}{1-\kappa} \right] \quad (48)$$

which has a peak at $\kappa \sim 1/\sqrt{2N}$. For $\kappa \ll 1$ this expression can be approximated by the simple function. Switching back to K it takes the form

$$f(K) \approx \frac{2K}{N} \exp \left[-\frac{K^2}{N} \right] \quad (49)$$

In Fig.8 we illustrate this distribution and demonstrate its applicability to the ring model.

We would like to point out that the analysis in this section is relevant to a random walk that is constrained to end up at the origin, $x(0) = x(N)$. Strictly speaking, the constrained random walk is the process that describes the potential $U(x)$. The maximal distance statistics of an unconstrained random walk is much different than an unconstrained random walk. This difference barely affects the barrier statistics.

MORE DETAILS ON SERIAL ADDITION

In the "site" notation, we have for the "conductance" between two sites

$$\vec{G} \equiv \left[\frac{1}{w_{\vec{1}}} + \frac{1}{w_{\vec{2}}} \left(\frac{w_{\vec{1}}}{w_{\vec{1}}} \right) \right]^{-1} \quad (50)$$

and similar expression for \overleftarrow{G}

$$\overleftarrow{G} \equiv \left[\frac{1}{w_{\overleftarrow{2}}} + \frac{1}{w_{\overleftarrow{1}}} \left(\frac{w_{\overleftarrow{2}}}{w_{\overleftarrow{2}}} \right) \right]^{-1} \quad (51)$$

We can repeat this procedure iteratively. If we have N bonds in series we get

$$\vec{G} = \left[\sum_{m=1}^N \frac{1}{w_{\vec{m}}} \exp \left(- \int_0^{m-1} \mathcal{E}(x) dx \right) \right]^{-1} \quad (52)$$

$$\overleftarrow{G} = \left[\sum_{m=1}^N \frac{1}{w_{\overleftarrow{m}}} \exp \left(\int_m^N \mathcal{E}(x) dx \right) \right]^{-1} \quad (53)$$

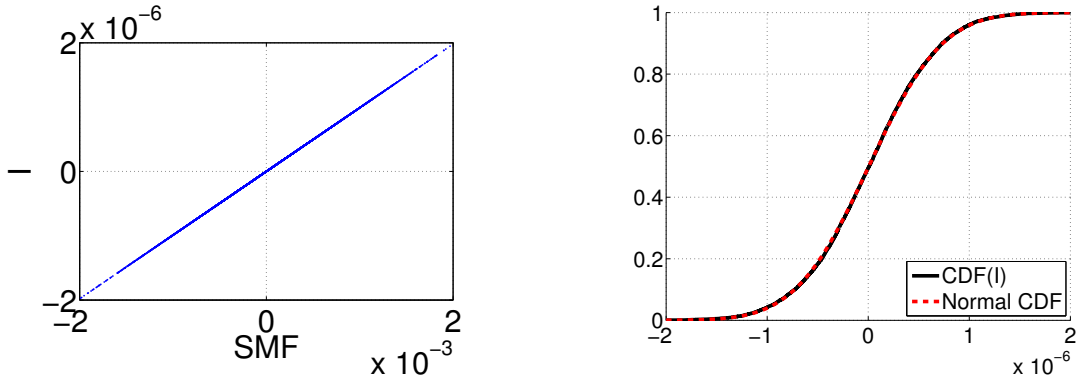


FIG. 6: In the linear regime, the current is strongly correlated with the SMF (left panel), and consequently it has *normal* statistics (right panel). For the statistical analysis we have generated 10^5 realizations of the ring with $\sigma = 6$.

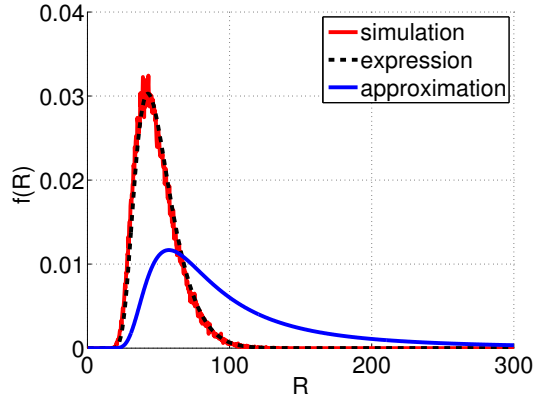


FIG. 7: Plot of $f(R)$. Red line is the outcome of a random walk simulation with $t = 1000$ steps that are Gaussian distributed with unit dispersion. The black dashed line is the exact result Eq.(43), while the blue solid line is from the simple asymptotic approximation Eq.(45).

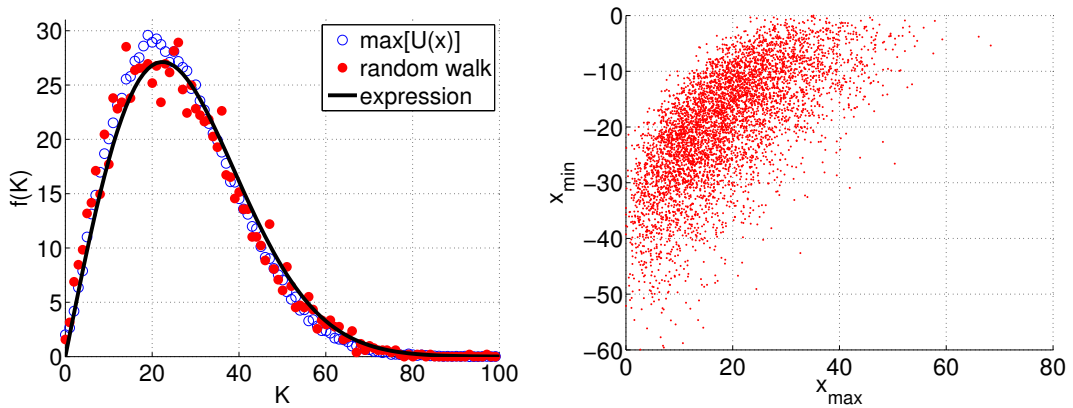


FIG. 8: [Left panel] Plot of $f(K)$. The histogram of $\max[U(x)]$ values over many ring realizations (blue circles) is compared with the K statistics in a constrained random walk process (red points). The analytical result Eq.(49) is represented by a black line. [Right panel] Scatter plot of maxima vs minima of constrained random walk, x_{\min} and x_{\max} are identically distributed, but strongly correlated.